Manipulating the Conductivity of Carbon-Black-Filled Immiscible Polymer Composites by Insulating Nanoparticles

Bo Li, Xiang-Bin Xu, Zhong-Ming Li, Yin-Chun Song

College of Polymer Science and Engineering, State Key Laboratory of Polymer Materials Engineering, Sichuan University, 127 YiHuanLu, NanYiDuan, Chengdu, 610065, Sichuan, People's Republic of China

Received 2 October 2007; accepted 15 April 2008
DOI 10.1002/app.28573
Published online 8 September 2008 in Wiley InterScience (www.interscience.wiley.com).

ABSTRACT: The conductivity of an immiscible polymer blend system, microfibrillar conductive poly(ethylene terephthalate) (PET)/polyethylene (PE) composite (MCPC) containing carbon black (CB), was changed by the addition of insulating $CaCO_3$ nanoparticles. In MCPC, the PET forms microfibrils during processing and PE forms the matrix. The CB particles are selectively localized in the PET microfibrils. When the insulating $CaCO_3$ nanoparticles are added, they substitute for some of the conductive CB particles and obstruct the electron paths. As a result, the resistivity of the MCPC can be tailored depending on the insulating filler content. The resistivity-insulating filler content curve displays a sluggish postpercolation region (the region immediately following the percolation region and in front of the equilibrium flat of the resistivity-filler content curve), suggesting that the MCPC in the postpercolation region possesses an enhanced manufacturing reproducibility and a widened processing window. These features are of crucial importance in making sensor materials. © 2008 Wiley Periodicals, Inc. J Appl Polym Sci 110: 3073–3079, 2008

Key words: carbon; polymer matrix composites; percolation; electrical conductivity

INTRODUCTION

Manufacturing reproducibility, that is, the immunity of a material's properties to fluctuation of both processing operations and parameters is of primary concern in producing conductive polymer composites (CPC). This is because the stable electrical properties of CPC materials give rise to the steady performance of the resulting electrical devices.[1,2] However, generally, the reproducibility of CPCs is not satisfied especially those in the practically valuable postpercolation region. The postpercolation region is defined as the region immediately after the percolation region of the resistivity-conductive filler loading curve and in front of the equilibrium flat, as shown in Figure 1. The resistivity of the samples in the postpercolation region maintains high sensitivity to environmental stimulation such as stress, gas, and heat due to immaturity of the conductive network. Also, the moderate resistivity of the samples leaves enough space for abrupt increase upon external stimulation.[1–4] These samples can thus serve as candidate materials for a variety of sensors such as chemical sensor, self-regulating heater, overcurrent protector, and heat detector.[1–8] However, for most CPC materials, this region is quite narrow, and after the percolation, the resistivity quickly transfers to an equilibrium flat as the loading of conductive fillers increases just a little. It has been well documented that the sharper this transition, the less reproducibility the material has, because the resistivity of the samples in this region can alter significantly even though a little vibration of processing parameters occurs during processing.[1] Thus, it is of great difficulties in making electrical devices with high precision based on these CPCs. To the opposite, the more sluggish this transition of the postpercolation region indicates the more enhanced reproducibility. The objective of this work is to slow down this transition and further widen the postpercolation region by manipulating the conductivity of the CPCs through a novel approach.

Up to now, only Zhang et al.[1] have performed a study on the postpercolation region to strengthen the reproducibility of the CPC material. They used the selective distribution of carbon black (CB) in the immiscible low-density polyethylene (PE)/ethylene-vinyl acetate copolymer blend. And a relatively flat portion was introduced in the postpercolation region

Correspondence to: Z.-M. Li (zmli@scu.edu.cn).
Contract grant sponsor: Nature Science Foundation of China; contract grant number: 50573049.
Contract grant sponsor: Programs for New Century Excellent Talents in University; contract grant number: NCET-04-0871.

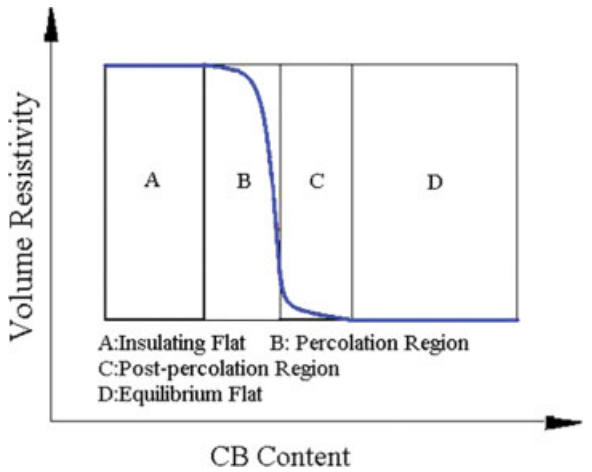

Figure 1 Regions of a volume resistivity-CB content curve, showing the definition of a postpercolation region. [Color figure can be viewed in the online issue, which is available at www.interscience.wiley.com.]

of the resistivity-CB-loading curve immediately after the first percolation region. The samples in this flat region had a strengthened reproducibility and a widened processing window, because the flat means that the resistivity of the composite was, to some extent, immune to the CB content vibration. Further increasing the CB content, another percolation behavior could be observed in this material due to the formation of conductive network at the interface. Although this two-step percolation method can lead to an adequate reproducibility, the introduction of the flat portion makes the conductivity unchangeable, which greatly limits the applications of such kind of material.

In this study, a specific immiscible polymer blend system, microfibrillar poly(ethylene terephthalate) (PET)/PE composite, was studied. The PET microfibrils were formed through a slit die extrution-hot stretching-quenching process, whereas PE formed the matrix phase. CB particles, the conductive filler, were selectively localized in the PET microfibrils to form a conductive network. By maintaining the volume ratio of CB : PET : PE and adding an insulating nanoparticle, nano-$CaCO_3$, the resistivity of the conductive microfibrillar composite can be tailored depending on the insulating filler content. In the previous work, it was well established that the surfaces of the CB-filled microfibrils played a key role in the conductivity of the composite.[9–12] The electron paths can only be conducted by effective connections, not only interconnection of microfibrils, but also interconnection of CB particles exposing on the surfaces of these microfibrils. And if the surface of fiber is smooth with well-covered plastics, the plastics coating the CB particles hinder the transport of electrons. Thus, only if the CB loading goes beyond the maximum packing fraction (Φ_{max}) of the CB particles in the PET microfibrils, which is defined as the maximum ratio of the volume of solids to the total volume, the CB particles can migrate to the surfaces of the microfibrils and then conduct the electron pathway of the composite. Current strategy is based on this specific conductive mechanism of the microfibrillar conductive polymer composite (MCPC). When nano-$CaCO_3$ was added into the microfibrils, the CB particles on the microfibrils' surfaces are gradually substituted by nano-$CaCO_3$. And nano-$CaCO_3$ particles play a similar role as the insulating polymer layer who obstructs the electron path way. Therefore, the gradually increased insulating area on the microfibrils' surfaces results in laggardly increased resistivity.

The choice of nano-$CaCO_3$ is motivated by the following reasons. First, both CB and insulating particle should have the preferential to localize in the PET phase to guarantee the substitution strategy. The selective distribution of CB in PET phase was warranted by our previous work. The fatty acid-treated surface of nano-$CaCO_3$ guarantees its better affinity to PET than PE. Second, it should be an insulating particle, which can obstruct conductive path. Third, the size of nano-$CaCO_3$ particle should be similar to that of CB. The bigger particles might influence the formation of microfibrillar, whereas the smaller ones might not be big enough to substitute the CB particles. Therefore, these properties of nano-$CaCO_3$ warrant the interaction of the two different particles inside the microfibrillar phase and further led to the controlled electrical properties.

EXPERIMENTAL

Materials

The main materials are nano-$CaCO_3$ (TB119, purchased from Inner Mongolia Mengxi Nano Material Limited-Liability Co., Neimenggu, China), CB (VXC-605, obtained from Cabot Co.), PET (a commercial grade of textile polyester, kindly donated by Luoyang Petroleum Chemical Co., Luoyang, China), and PE (5000S, purchased from Daqing Petroleum Chemical Co., Daqing, China). The specific physical parameters of these materials have been reported elsewhere,[9] except nano-$CaCO_3$. The nano-$CaCO_3$ was treated by the fatty acid with a particle size ranging from 20 to 30 nm, and a density ranging from 2.5 to 2.6 g/cm^3. The solvent used to premix CB and nano-$CaCO_3$ was ethanol (analytically pure 99.7%) purchased from Kelong Co., Chengdu, China.

Sample preparation

Premixing of the fillers

The fillers, CB and nano-$CaCO_3$, were first mixed in solvent (ethanol) under ultrasonic water bath (80°C), and mechanical stirring to fabricate homogeneous filler mixture. The filler mixture together with ethanol was stirred for 10 min in the three-necked bottle located in the ultrasonic water bath, and then the ethanol was quickly evaporated under the aid of a vacuum pump. The residue was further dried at the temperature of 120°C for 24 h to remove the remaining solvent.

Preparation of masterbatch of microfibrillar phase

The filler mixture was then compounded with PET pellets in an internal mixer to fabricate the masterbatch of the microfibrillar phase under the temperature of 270°C. The PET pellets were first filled into the internal mixer for 5 min. And then the filler mixture was put into the internal mixer for another 5 min to fabricate the CB/nano-$CaCO_3$/PET masterbatch. The resulting agglomerates were further crashed into small particles.

Extrusion and hot stretching of the composites

The obtained CB/nano-$CaCO_3$/PET particles and PE pellets were mixed in a single extruder (with a screw length to diameter, *L/D*, of 30) and extruded through a slit die (15 mm wide, 2 mm high); the extruded melting strip was then stretched by a taking up device with two pinching rolls to *in situ* form the CB/$CaCO_3$/PET microfibrils. The stretched strip was then quenched in a cold water bath to stabilize the microfibrillar morphology. The temperature profile used for the extruder was 190, 250, 280, and 270°C from hopper to die, the roll temperature maintained 40°C, and the temperature of cold water bath is 20°C. The hot stretch ratio (the ratio of the area of transverse section of slit die to the area of transverse section of strip) of the strip is calculated to be 11.8.

Compression molding of sample plaques

The resulting strips were cut into small pieces and then compression molded into plaque samples with the dimension of 2 × 100 × 100 mm for electrical property tests. The procedures were as follows: the materials were first hot-pressed for 10 min under the pressure of 5 MPa and then cold-pressed for 5 min under the same pressure. The temperature during the hot-pressing maintained 150°C, whereas the temperature for cold pressing is about 20°C.

TABLE I
The Volume Ratio of Components and the Volume Resistivities from S1 to S6

Sample	CB/nano-$CaCO_3$/PET/PE	Volume resistivity (Ω × cm)
S1	11/0/75/241	2.44×10^4
S2	11/7/75/241	5.06×10^4
S3	11/14/75/241	2.05×10^5
S4	11/21/75/241	1.28×10^6
S5	11/28/75/241	1.40×10^{15}
S6	11/35/75/241	1.96×10^{15}

The volume ratio of CB, PET, and PE maintained 11 : 75 : 241 throughout this work. By adding different fractions of nano-$CaCO_3$, as shown in Table I, a series of samples with different nano-$CaCO_3$ contents were obtained from S1 to S6, having the CB/nano-$CaCO_3$ volume ratios of 11 : 0, 11 : 7, 11 : 14, 11 : 21, 11 : 28, and 11 : 35, respectively.

To observe the dispersion state of the particles, a strip of S3 was cryofractured in the liquid nitrogen. The cryofractured surface was sputter coated with gold particles and further photographed using a JEOL JSM-5900LV Scanning Electron Microscope (SEM). SEM was also used to observe the morphology of the dispersed phase after the PE matrix was etched away by xylene, and the extruded strips of samples S1, S3, and S6 were involved in this observation. The treatment was as follows: first, the sample strips were put into hot xylene (125°C) for 15 h, and the solvent was refreshed every 5 h; second, the strips were dried in the oven for 8 h at the temperature of 80°C. After the treatment, the microfibrils exposed on the surface can be easily observed. Additionally, for the samples that cannot maintain the shape of strip during this treatment, the residues in the solvent were collected and dried for further test.

Resistivity testing

A two-point probe method was adopted to test the resistivity of the insulating samples, and a high resistivity meter model ZC-36 was applied with a voltage of 100 V. For the samples with resistivity lower than 10^8 Ω × cm, a four-point method (ASTM D-991) was applied by using two DT9205 digital multimeters and a voltage supply.

RESULT AND DISCUSSION

Results

SEM observation of MCPC

Figure 2 shows the cryofractured surface of sample S3. A cross section of a fractured microfibril and a pulled out tip of another microfibril embedded in

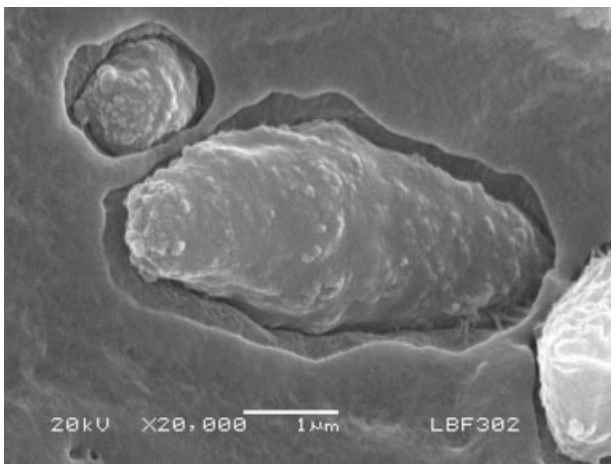

Figure 2 High magnification SEM micrograph of cryofractured surface of S3, in which volume ratio of CB/nano-$CaCO_3$ equals 11 of 14.

the smooth cryofractured surface of the PE matrix can be seen. Almost all the particles, including both CB particles and nano-$CaCO_3$ particles, are localized either inside the microfibrils or on the surface of microfibrils. Figure 3(a–c) shows the morphology evolvement of the microfibrillar composite as a function of the nano-$CaCO_3$ content. In S1 [Fig. 3(a)], without nano-$CaCO_3$, the well-defined fibrils with smooth surfaces appear aligning almost in one direction (flow direction) (the diameters of the microfibrils have the range of 1–10 μm, with an average length of more than 150 μm). As the nano-$CaCO_3$/CB volume ratio increases to 14 : 11(S3), shown in Figure 3(b), the fibrils become thicker and their surfaces turn rougher. When the volume ratio of nano-$CaCO_3$/CB reaches 35 : 11(S6) [Fig. 3(c)], PET cannot maintain microfibrillar morphology, but assumes irregular domains. Figure 4 exhibits the detailed structure information of microfibrils' surfaces. When compared with Figure 4(a), more particles expose on the surface of microfibril in Figure 4(b), along with the increase of the nano-$CaCO_3$ content from S1 to S3. Also, the microfibril in Figure 4(b) shows a much coarser surface, and due to the increase of the total filler content, and the shape of the microfibril is not as regular as that in Figure 4(a).

Resistivity of MCPC

Figure 5 depicts the volume resistivity of the composite as a function of nano-$CaCO_3$ mass fraction in the microfibril phase. It is interesting that the resistivity experiences a very slow increase from 2.44×10^4 to 1.28×10^6 $\Omega \times$ cm, although the nano-$CaCO_3$ in the microfibril phase (CB/nano-$CaCO_3$/PET) greatly increases from 0 up to 30.81 wt %, corresponding to S1 and S4. Here, it should be noted that, for the ease of plotting and comparison, here the volume ratios in the microfibrillar phase were changed to the mass fractions. Further adding insulating nano-$CaCO_3$, however, the volume resistivity increase rapidly, being analogous to a conventional percolation behavior in the filled CPC as a result of changing the conductive filler loading.[10] In fact, although the insulating nano-$CaCO_3$ loading

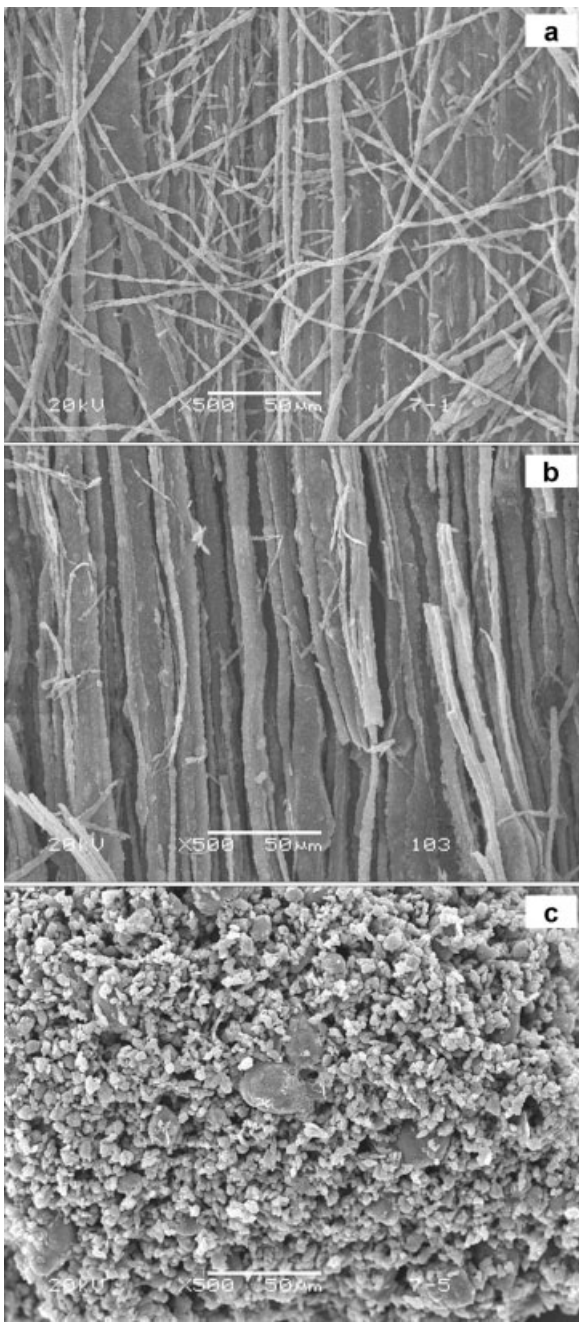

Figure 3 SEM micrographs of microfibril morphology evolvement in MCPC strips S1 (a), S3 (b), and S6 (c), prepared by etching away the PE matrix on the surface of the MCPC strips in hot xylene. The volume ratios of CB/nano-$CaCO_3$ in S1, S3, and S6 are 11/0, 11/14, and 11/35, respectively.

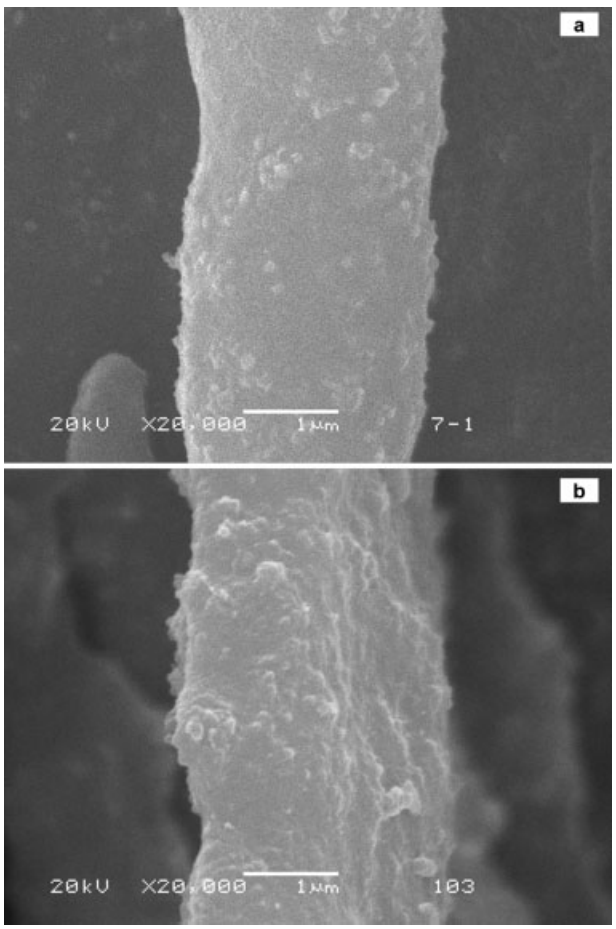

Figure 4 High magnification SEM micrographs of surface of microfibrillar in sample strips, S1 (a), S3 (b), prepared by etching away the PE matrix on the surface of the MCPC strips in hot xylene.

increases, the true CB content in the composite gradually decreases. However, in MCPC, both matrix polymer and microfibrillar phase polymer constitute most of the volume fraction, and even though the volume ratio of microfibrillar phase (CB/nano-$CaCO_3$/PET) changes a lot, the volume fraction of CB in the composite changes only a little. As shown in the insert figure of Figure 5, a zig-zag drop of the resistivity can be seen as a function of the CB volume fraction in the composite. The volume fraction of CB only ranges from 3.04 to 3.36 vol %.

Discussion

The earlier results show that the morphology evolvement of dispersed phase and the changing surface condition of microfibrils are both dependent on the nano-$CaCO_3$ content. In the postpercolation region, by gradually increasing the nano-$CaCO_3$ content, from 12.92 wt % (7.52 vol %) to 30.81 wt % (19.63 vol %) in the microfibrillar phase, the morphology and structure of the MCPC underwent a great change. As a result, the resistivity of the samples can be tailored, because it strongly depends on its morphology and structure, as discussed below. And a sluggish transition and a widened processing window based on nano-$CaCO_3$ have thus been obtained.

Concerning the exact mechanism of this sluggish transition, a series of factors have to be taken into consideration, including the selective distribution of the fillers, maximum packing fraction of microfibril phase, and the specific conductive mechanism of the MCPC.

The selective distribution of both particles as testified in Figure 2 is of crucial importance. The preferential localization of CB particles in immiscible polymer blends has been reported in some literature.[9–17] The key factors controlling the preferential distribution of CB particles are the interfacial tension between CB and polymer components, the viscosity of the polymer components, order of mixing, etc. According to the previous work,[11] the CB particles interact strongly with the PET phase than with PE phase, with interfacial tensions of 5.89 and 13.1 mN/m, respectively. Moreover, the premixing of CB with PET phase strengthens CBs' selective distribution in PET, because of the thermodynamic nature of particles, which prevents CB from emigrating to PE phase. Combined these two factors mentioned earlier, the selective distribution of CB particles in PET phase is warranted. The similar condition happened to nano-$CaCO_3$. On one hand, the fatty acid surface of nano-$CaCO_3$ can interact with ester group in the PET chain and thus enhance the interaction between nano-$CaCO_3$ and PET; on the other hand, the premixing technology enhances the effect of selective distribution. In the high magnification SEM image,

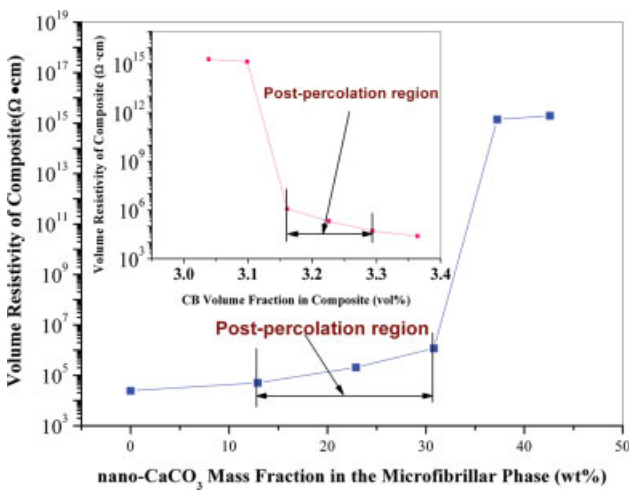

Figure 5 Volume resistivity versus mass fraction of nano-$CaCO_3$ in the microfibrillar phase (CB/nano-$CaCO_3$/PET). Insert: volume resistivity versus volume fraction of CB in the composite. [Color figure can be viewed in the online issue, which is available at www.interscience.wiley.com.]

as shown in Figure 2, the sharp contrast at the interface of microfibrillar phase and matrix proved that all the particles were localized in the microfibrillar phase. Even though the particles were overloaded in the microfibrillar phase, they did not further step into matrix, but chose to localize at the interface.

However, it is not warranted to say that $CaCO_3$ particles without surface treatment could not disperse in the PET. The heterogeneous distribution of particles is dictated by the surface condition of particles[14] and the interfacial tension among particles and different polymer phases.[15] Therefore, without the acid group on the surface of $CaCO_3$ particles, the surface condition as well as the interfacial tension should be analyzed to determine the distribution of these particles. However, this is of main concern of this manuscript. Further work will be done to figure out this problem.

Given that both CB and nano-$CaCO_3$ prefer to localize in the PET phase, along with the increase of filler content, these two kinds of particles begin to rival for limited space of the microfibrillar phase. When the fillers' content reaches the maximum packing fraction (Φ_{max}), the fillers begin to migrate to the interfaces. As shown in Figure 4(a,b), the surface morphology of microfibril is closely related to the filler content, and the more filler content, the more coarser the surface of microfibril. The conductive mechanism of MCPC[9] indicates that the surface condition of the microfibril dictates the resistivity of the final samples. Along with the increasing nano-$CaCO_3$ content, more particles are exposing on the surface. In the postpercolation region, the CB particles on the surface of microfibrils do exist, because the conductive pathway can only be conducted by these particles. However, it is not clear whether CB particles have the priority to localize on the surface or not, compared to nano-$CaCO_3$ particles. If CB has the priority, although nano-$CaCO_3$ prefers to localize in the center of the microfibril, an increased conductivity is expected. Along with the increase of nano-$CaCO_3$, more and more CB particles are forced to migrate to the surface, and the increasing conductive particles on the surface increase the possibility of effective connection. However, the experimental results show the opposite tendency. This tendency indicates that compared to nano-$CaCO_3$, CB particles do not have that priority. The component of the filler on the surface is closely related to the original ratio of CB/nano-$CaCO_3$. By increasing the content of nano-$CaCO_3$ gradually, nano-$CaCO_3$ particles substitute the CB particles on the surface of microfibrils step by step. The insulating fillers on the surface of microfibrils hold back the transport of electrons, and thus more and more electron paths are obstructed by insulating particles. Accordingly, the resistivity of the postpercolation region increase gradually.

Although there are few articles aiming at the resistivity control in the postpercolation region, several methods have been developed dealing with the percolation region.[5,18,19] The objectives of these methods are to retard or even eliminate the percolation region. And the physical and structural parameters of the conductive particles such as the dispersion state, particle size, particle morphology, and the surface energy are key factors in controlling. For example, Ando and Takeuchy[18] changed the dispersion state of CB in the nature rubber, by grafting the CB particles with methyl isobutyl ketone, ethylene glycol macromer, styrene, and isopropenyl oxazoline, and a gradually reduced resistivity-CB loading curve can be obtained. Also, Chan[5] gained a similar result by changing the particle size through a premixing method to fabricate compound filler with a larger particle size. Sumita et al.[19] addressed the importance of surface energy of CB particles, and by fluorinating the surfaces of CB particles, both theoretical prediction and experimental result showed a retarded curve. However, the pretreatments of particles in these methods increase the cost of materials, consume a lot of energy, and jeopardize the conductivity of the final product. Moreover, these methods mainly deal with the percolation region, which has little application potential in sensor material for its high resistivity. To the opposite, the insulating filler used in our method is much cheaper, and the energy of pretreatment is also saved. Also, our method has strong maneuverability, because the two steps processing can be accomplished by traditional processing methods and the ratio of CB, nano-$CaCO_3$, and PET can be easily controlled, because the content of nano-$CaCO_3$ varies over a wide range.

It is also interesting that the percolation behavior of this CB and $CaCO_3$-filled MCPC may be not a content dependent percolation, but a morphology-dependent one. On one hand, the percolation region of CB content is too narrow, only 0.06 vol %, as shown in the insert figure of Figure 5, which has never been reported in any reference. The efficiency of CB as a conductive filler is not as high as that by increasing such a little amount, the resistivity can reduce so greatly. On the other hand, as shown in Figure 3, the morphology of microfibrillar phase changes greatly when the percolation happens. Increasing the filler content leads to the breakdown of microfibrillar morphology and then the amorphous blocks with much surface covered with nano-$CaCO_3$ cannot form a throughout conductive network. This limitation implies that if the microfibrillar phase can be maintained to a higher filler loading, a wider postpercolation region is expected.

The breakdown of microfibrillar morphology is caused by the greatly increased viscosity of PET phase. The fibrillation capability of the PET in the

composite depends not only on the elongational flow field during hot stretching, but also on the particle loading.[10,11] In this work, the volume ratio of CB/PET/PE was fixed as 11 : 75 : 241, and the share of nano-$CaCO_3$ varied from 0 to 35. The keeping increase of nano-$CaCO_3$ will fill in the limited space of dispersed phase (PET), which makes the viscosity of PET higher and higher, verified by the fact that the surface of PET microfibrillar turns coarse as the increase of nano-$CaCO_3$, as shown in Figure 4(a,b). When the viscosity of the PET reaches beyond a critical value, the PET phase cannot be deformed into microfibrillar morphology, but amorphous blocks.

CONCLUSIONS

Using an insulating nanoparticle, the electrical properties of MCPC in the postpercolation region can be effectively tailored, and the postpercolation can be greatly widened. Thus, this CPC material can serve as a candidate for multifunctional sensors with enhanced reproducibility. This is a method with low cost and good accessibility. Furthermore, this is a novel idea on the property control of conductive immiscible polymer blend. The future issues will be concentrated on the applications of this material and optimizing the controllability of this method.

The authors thank Mr. Zhu Li from Analytical and Testing Center of Sichuan University for his help in the SEM observation.

References

1. Zhang, M. Q.; Yu, G.; Zeng, H. M.; Zhang, H. B.; Hou, Y. H. Macromolecules 1998, 31, 6724.
2. Sisk, B. C.; Lewis, N. S. Langmuir 2006, 22, 7928.
3. Narkis, M.; Ram, A.; Flashner, F. Polym Eng Sci 1978, 18, 649.
4. Narkis, M.; Ram, A.; Flashner, F. J Appl Polym Sci 1978, 22, 1163.
5. Chan, C. M. Polym Eng Sci 1996, 36, 495.
6. Lonergan, M. C.; Severin, E. J.; Doleman, B. J.; Beaber, S. A.; Grubbs, R. H.; Lewis, N. S. Chem Mater 1996, 8, 2298.
7. Segal, E.; Tchoudakov, R.; Mironi-Harpaz, I.; Narkis, M.; Siegmann, A. Polym Int 2005, 54, 1065.
8. Chen, J. H.; Tsubokawa, N. Polym Adv Technol 2000, 11, 101.
9. Xu, X. B.; Li, Z. M.; Yang, M. B.; Jiang, S.; Huang, R. Carbon 2005, 43, 1479.
10. Li, Z. M.; Xu, X. B.; Lu, A.; Shen, K. Z.; Huang, R.; Yang, M. B. Carbon 2004, 42, 428.
11. Xu, X. B.; Li, Z. M.; Yu, R. Z.; Lu, A.; Yang, M. B.; Huang, R. Macromol Mater Eng 2004, 289, 568.
12. Xu, X. B.; Li, Z. M.; Dai, K.; Yang, M. B. Appl Phys Lett 2006, 89, 032105.
13. Sumita, M.; Sakata, K.; Ami, S.; Miyasaka, K.; Nakagawa, H. Polym Bull 1991, 25, 265.
14. Wu, G. Z.; Asai, S.; Sumita, M.; Yui, H. Macromolecules 2002, 35, 945.
15. Wu, S. Polymer Interface and Adhesion; New York: Marcel Dekker, 1982; p 98.
16. Khan, C.; Kubht, J. J Appl Polym Sci 1975; 19: 831.
17. Gubbels, F.; Jérôme, R.; Teyssié, Ph.; Vanlathem, E.; Deltour, R.; Calderone, A.; Parenté, V.; Brédas, J. L. Macromolecules 1994, 27, 1972.
18. Ando, N.; Takeuchi, M. Thin Solid Films 1998, 334, 182.
19. Katada, A.; Buys, Y. F.; Tominaga, Y.; Asai, S.; Sumita, M. Colloid Polym Sci 2005, 283, 367.